EXPERIMENT 21

NMR Study of a Reversible Hydrolysis Reaction

The hydrolysis of pyruvic acid to 2,2-dihydroxypropanoic acid is a reversible reaction giving rise to the following equilibrium in aqueous solution:

$$CH_3COCOOH + H_2O \underset{k^r}{\overset{k^f}{\rightleftharpoons}} CH_3C(OH)_2COOH \qquad (1)$$

In this experiment, nuclear magnetic resonance (NMR) techniques will be used to determine the specific rate constants k^f and k^r for the forward and reverse reactions as well as the value for the equilibrium constant K. Like the hydrolysis of many other organic compounds, this reaction can be acid catalyzed and the effect of hydrogen-ion concentration on the kinetics can be studied. Furthermore, the dependence of k^f, k^r, and K on temperature will be measured and used to evaluate activation energies.

THEORY

A first-order reaction is ordinarily understood to be one in which the rate of disappearance of a single species is proportional to the concentration of that species in the reaction mixture. This terminology is often used even when strictly speaking the total reaction order is different from unity, owing to the participation of additional species in the reaction that are themselves not consumed (i.e., catalysts—H^+ in the present instance) or the participation of substances that are present in such large amounts that their concentrations do not undergo significant percentage change during the reaction (H_2O in the present instance). It would be more correct in such cases to state that the reaction is first-order with respect to a given disappearing species.

The reversible pyruvic acid hydrolysis proceeds kinetically along both an uncatalyzed and an acid-catalyzed path:

Path I

$$CH_3\overset{\overset{O}{\|}}{C}-COOH + H_2O \underset{k_0^r}{\overset{k_0^f}{\rightleftharpoons}} CH_3\overset{\overset{OH}{|}}{\underset{\underset{OH}{|}}{C}}-COOH \qquad (2)$$

Path II

$$CH_3\overset{\overset{O}{\|}}{C}-COOH + H^+ \rightleftharpoons CH_3\overset{+}{C}\underset{\underset{OH}{|}}{}-COOH \qquad \text{very rapid to equil. } K_1 \qquad (3)$$

$$CH_3\overset{+}{C}\underset{\underset{OH}{|}}{}-COOH + H_2O \underset{k_1^r}{\overset{k_1^f}{\rightleftharpoons}} CH_3\overset{\overset{OH}{|}}{\underset{\underset{OH}{|}}{C}}-COOH + H^+ \qquad (4)$$

Introducing an abbreviated notation for convenience such that A = $CH_3COCOOH$, B = $CH_3C(OH)_2COOH$, and AH^+ = $CH_3C^+(OH)COOH$, one finds

$$+\frac{d(\mathrm{B})}{dt} = k_0^f(\mathrm{A}) - k_0^r(\mathrm{B}) \qquad \text{for path I} \tag{5}$$

$$+\frac{d(\mathrm{B})}{dt} = k_1^f(\mathrm{AH}^+) - k_1^r(\mathrm{H}^+)(\mathrm{B}) \tag{6a}$$

$$= k_1^f K_1(\mathrm{H}^+)(\mathrm{A}) - k_1^r(\mathrm{H}^+)(\mathrm{B}) \tag{6b}$$

$$= k_\mathrm{H}^f(\mathrm{H}^+)(\mathrm{A}) - k_\mathrm{H}^r(\mathrm{H}^+)(\mathrm{B}) \qquad \text{for path II} \tag{6c}$$

where (X) denotes the concentration of species X. In Eqs. (5) and (6*a*), the quantity (H_2O), which is constant, has been incorporated into k_0^f and k_1^f, respectively. Equation (6*b*) has made use of the equilibrium approximation $K_1 = (\mathrm{AH}^+)/(\mathrm{A})(\mathrm{H}^+)$ for reaction step (3). The overall rate of change in (B) is given by the pseudo-first-order expression

$$+\frac{d(\mathrm{B})}{dt} = k^f(\mathrm{A}) - k^r(\mathrm{B}) \tag{7}$$

where

$$k^f = k_0^f + k_\mathrm{H}^f(\mathrm{H}^+) \tag{8a}$$

$$k^r = k_0^r + k_\mathrm{H}^r(\mathrm{H}^+) \tag{8b}$$

When reaction (1) achieves equilibrium, the thermodynamic equilibrium constant K is given by

$$K = \frac{(\mathrm{B})_\mathrm{eq}}{(\mathrm{A})_\mathrm{eq}} \tag{9}$$

and the principle of detailed balancing[1] then yields

$$\frac{d(\mathrm{B})}{dt} = k_0^f(\mathrm{A})_\mathrm{eq} - k_0^r(\mathrm{B})_\mathrm{eq} = 0 \qquad \text{for path I}$$

$$K = \frac{k_0^f}{k_0^r} \tag{10a}$$

and

$$\frac{d(\mathrm{B})}{dt} = k_\mathrm{H}^f(\mathrm{H}^+)(\mathrm{A})_\mathrm{eq} - k_\mathrm{H}^r(\mathrm{H}^+)(\mathrm{B})_\mathrm{eq} = 0 \qquad \text{for path II}$$

$$K = \frac{k_\mathrm{H}^f}{k_\mathrm{H}^r} \tag{10b}$$

Dependence on Temperature. The effect of temperature on specific rate constants is well described by the Arrhenius expression

$$k = A \exp\left(-\frac{E_a}{RT}\right) \tag{11}$$

where A is a temperature-independent *frequency factor* and E_a is an activation energy, interpretable as the energy required to reach the transition state or *activated complex.*

Arrhenius plots of $\ln k$ versus $1/T$ should yield a straight line with a negative slope, and the activation energies for the forward and reverse reactions are given by

$$E_a^f = -R\frac{d \ln k^f}{d(1/T)} \qquad E_a^r = -R\frac{d \ln k^r}{d(1/T)} \tag{12}$$

In addition, the effect of temperature on the equilibrium constant K is governed by the Gibbs–Helmholtz equation,

$$\frac{d \ln K}{d(1/T)} = -\frac{\Delta\tilde{H}^0}{R} \tag{13}$$

where $\Delta\tilde{H}^0$ is the molar standard enthalpy change for the reaction. It follows from Eqs. (10) to (13) that

$$\Delta\tilde{H}^0 = E_a^f - E_a^r \tag{14}$$

METHOD

The use of NMR techniques to investigate the present system is based on an experiment first described in Ref. 2. Two quantitative aspects of NMR spectra are involved. The first is the familiar fact that the integrated band area is directly proportional to the concentration of nuclei that give rise to that band. Thus the equilibrium constant K can be obtained from the ratio of integrated band areas for $CH_3C(OH)_2COOH$ (species B) and $CH_3COCOOH$ (species A). The second aspect, concerning the dynamic information that can be obtained from band-shape analysis, is less familiar and will be summarized below.

For an idealized case (perfectly homogeneous magnet, low transverse fields, steady-state conditions, no saturation effects), an NMR absorption line in the frequency domain or the Fourier transform of a free induction decay has a Lorentzian profile[3]

$$I(\nu) = \frac{I_0}{1 + 4\pi^2(\nu - \nu_0)^2 T_2^2} \tag{15}$$

When $\nu = \nu_0$, which corresponds to the resonance condition where the frequency of the field matches the Larmor frequency ν_0, the intensity achieves its maximum value $I_0 = CT_2$.[4] The constant C depends on several nuclear and instrumental parameters that do not vary in a given experiment. An ideal Lorentzian line shape is characterized by a full-width-at-half-maximum (FWHM) W given by

$$W(\text{Hz}) = \frac{1}{\pi T_2} \text{ (ideal)} \tag{16}$$

since $I(\nu) = I_0/2$ at $\nu = \nu_0 \pm (2\pi T_2)^{-1}$. The quantity T_2 is called the *spin-spin relaxation time* or the *transverse relaxation time*, since it governs the decay of the transverse magnetization $M_y(t) \sim \exp(-t/T_2)$.

Typical proton NMR T_2 values are of the order of 1 s, so $W \simeq 0.3$ Hz would be expected if there were no chemical exchange and no instrumental contributions to W. However, there are always small magnetic field inhomogeneities that spread the Larmor frequencies slightly. If one assumes that the line shape remains Lorentzian, Eq. (15) can easily be modified by replacing T_2 with an effective value T_2^*, where

$$W(\text{Hz}) = \frac{1}{\pi T_2^*} = \left(\frac{1}{\pi T_2}\right) + W_{\text{inst}} \tag{17}$$

and T_2^* reflects the instrumental contribution as well as the natural line width.[3,5]

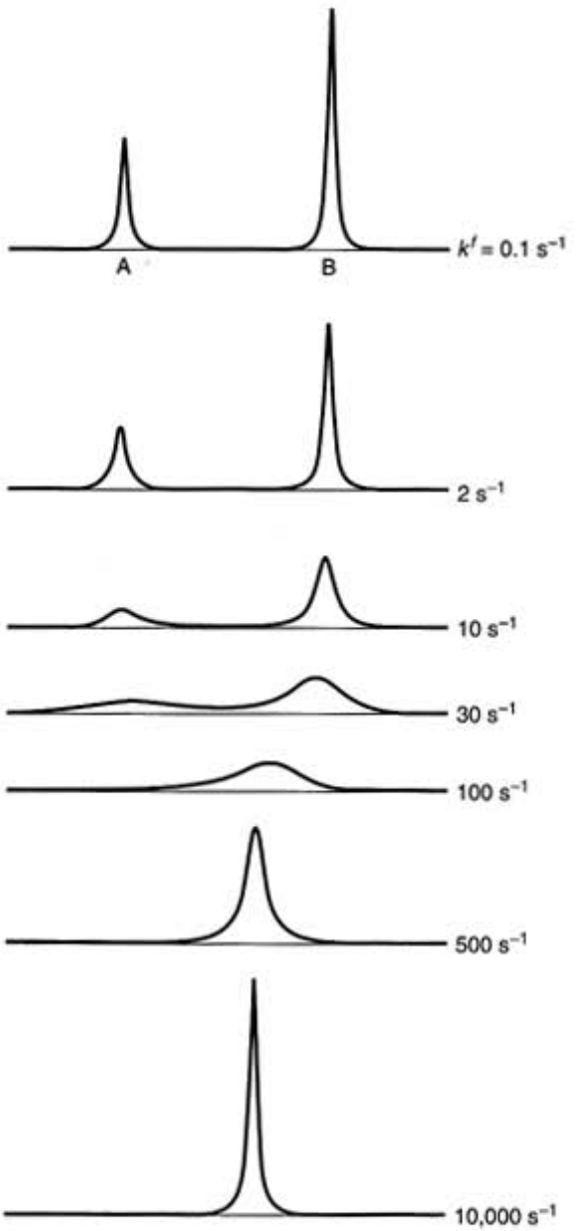

FIGURE 1
Changes in the NMR spectrum for a two-site exchange system as a function of $k^f = k_{A\to B}$. Model parameters used: $K = (B)/(A) = 2$, $\nu_A - \nu_B = 20$ Hz, and $T_{2A}^* = T_{2B}^* = 0.5$ s.

Chemical Exchange. If the chemical system under investigation contains magnetic nuclei that can transfer rapidly between two different environments, this chemical exchange can have dramatic effects on the NMR spectrum. In our case, the methyl protons occupy site A in pyruvic acid and site B in dihydroxypropanoic acid, and they switch back and forth due to the reversible hydrolysis reaction. The general equations for two-site exchange are fairly complex,[4,6] but the qualitative changes in the spectrum due to $A \rightleftharpoons B$ exchange are shown in Fig. 1. At slow exchange rates (small values of k^f and k^r), two nonoverlapping lines are observed with FWHM values W_A and W_B given by

$$\pi W_A = \frac{1}{T_{2A}^*} + k^f \qquad \pi W_B = \frac{1}{T_{2B}^*} + k^r \tag{18}$$

Thus, for very small rate constants, the widths are dominated by the effective T_2^* values that would pertain in the absence of exchange. In this limit the mean lifetimes $\tau_A = 1/k^f$ for a nucleus in environment A and the analogous $\tau_B = 1/k^r$ for environment B are long compared to the time required for a magnetic transition, and both lines are "sharp." As k^f (and $k^r = k^f/K$) increases due to changes in (H^+) or temperature, the lines grow wider. If k^f grows sufficiently large, the lines become very broad and overlap, then merge into a single line, and this line becomes progressively sharper as k^f continues to increase, as shown in Fig. 1. The initial broadening of the lines described by Eq. (18) is an example of lifetime broadening[2,5] that follows from the Heisenberg uncertainty principle in the form $\Delta E \cdot \Delta t \simeq h/2\pi$. In our case, since $\Delta E = h\Delta\nu$ and $\Delta t = \tau$, this condition is $\Delta\nu \cdot \tau \simeq 1/2\pi$ and therefore $W = 2\Delta\nu \simeq 1/\pi\tau$.

EXPERIMENTAL

Descriptions of the general features of continuous-wave NMR (CW–NMR) and Fourier-transform NMR (FT–NMR) spectrometers are given in Exps. 32 and 43, respectively. The instructor will provide specific operating procedures for the particular instrument to be used in this experiment and will suggest choices of operational parameters such as sweep rates (CW spectrometer) or acquisition times (FT spectrometer). The shimming of the NMR probe to achieve the narrowest possible line width (smallest W_{inst}) is important and should be practiced on some convenient reference sample, perhaps pure pyruvic acid. It is also essential to obtain expanded-scale spectra, and care should be taken that enough digitized data points are acquired across a peak to allow an accurate determination of integrated band areas and widths. It should be stressed that high-quality spectra with optimal resolution are required, and the radio-frequency (B_1) field should be well below saturation levels.[4]

Pyruvic acid is hygroscopic and may polymerize or decompose somewhat on standing at room temperature; impure samples are yellowish. A supply of pyruvic acid should be purified in advance by vacuum distillation to remove water, decomposition products, and any other impurities. With the use of a laboratory pump, this distillation can be carried out anywhere between 20 and 50°C depending on the pressure achieved. Be sure to add boiling chips or use a magnetic stirrer (better at lower pressures) to prevent bumping. The distilled material should be a clear, colorless liquid. Store the purified pyruvic acid in an airtight container in a refrigerator. If solutions are made up in advance, they should also be stored in small sealed tubes kept in a refrigerator. Under such conditions, solutions should remain sufficiently stable for 4 or 5 days.

Prepare the solutions listed in Table 1. The HCl is reagent-grade concentrated hydrochloric acid containing ~38 percent HCl by weight (about 12 *M*). Note that the solvent consists of a mixture of H_2O and D_2O, the latter added to provide a NMR lock.

TABLE 1

Soln.	Pyruvic Acid, mL	HCl, mL	H_2O, mL	D_2O, mL
1	1.0	0	1.10	0.10
2	1.0	0.10	1.00	0.10
3	1.0	0.20	0.90	0.10
4	1.0	0.30	0.80	0.10
5	1.0	0.40	0.70	0.10
6	1.0	0.50	0.60	0.10

The concentration of D_2O is fixed at the same value for all the solutions in order to hold constant any possible isotope effect on the rates. **Caution:** Since pyruvic acid is irritating to the skin and concentrated HCl can cause severe burns, solution handling should be carried out wearing gloves.

Each solution should be prepared in a small test tube or vial that can be sealed airtight for refrigerated storage prior to transfer to an NMR sample tube. In order to calculate the H^+ concentration in each solution, the molarity of the concentrated HCl is needed. If this is not given by the instructor, it can be determined either by titration or by a density measurement (using tables in the *CRC Handbook of Chemistry and Physics*).

The NMR spectrum of pure pyruvic acid consists of two resonances—one due to the carboxyl proton at 8.67 ppm and another due to methyl protons at 2.55 ppm (relative to tetramethylsilane as the reference).[7] The separation between these two peaks is dependent on the purity of the sample—the greater the purity, the greater is the separation. Taking the spectrum of pyruvic acid will allow a qualitative check on sample purity and will also provide practice with shimming a sample for optimal resolution (narrow lines).

The spectrum of an aqueous solution of pyruvic acid consists of a total of three bands for the species involved in the equilibrium given by Eq. (1). The methyl protons of pyruvic acid give a band A with a chemical shift $\delta_A = 2.6$ ppm; and the methyl proton band for dihydroxypropanoic acid, denoted band B, occurs at $\delta_B = 1.75$ ppm. A third band at a larger δ value represents the resonances of the carboxyl, hydroxyl, and water protons. This band is a singlet since the proton exchange rate between —COOH, —OH, and H_2O environments is very rapid. The positions of all three bands will vary somewhat with the composition of the solution.

Dependence on Hydrogen-Ion Concentration. Solutions 1 through 6 will be studied at a constant temperature of 25°C in order to determine the acid-catalyzed rate constants k_H^f and k_H^r. If the NMR sample tubes have been filled with cold solutions, bring these tubes up to room temperature before inserting them into the spectrometer and allow about 5 min for the tubes to come to thermal equilibrium with the probe. You should then lock on and shim each sample tube to achieve the narrowest possible line widths.

The two methyl peaks should be recorded on an expanded scale in order to achieve good width measurements. As the H^+ concentration changes, the peak positions will shift appreciably and it will probably be necessary to change the screen scan parameters. Integrate the band area for each peak and determine the widths W_A (for pyruvic acid) and W_B (for dihydroxypropanoic acid). As these data are being obtained, make preliminary plots of line widths versus the hydrogen-ion concentration. These plots should be linear, as indicated by Eq. (19) in the Calculations section. If the points for any of the samples deviate substantially from the linear trend of the other data points, this is probably due to improper shimming and you should reshim that sample and repeat the measurements.

Temperature Dependence of Uncatalyzed Rate. The line widths and band areas for solution 1 (containing no HCl) will be measured as a function of temperature over the range 45 to 65°C. This will allow a determination of the T dependence of the equilibrium constant K and an approximate evaluation of the activation energies for the forward and reverse reactions.

Reinstall sample tube 1 in the spectrometer and adjust the probe temperature controller to 45°C. After the sample has reached 45°C (~10 min), relock and reshim the sample. This shim setting will be maintained for all the temperature runs. Once the methyl spectrum has been recorded and plotted on an expanded scale and the determination of integrated band areas and FWHM line widths has been completed at 45°C, raise the temperature by 5°C intervals and repeat the process until you reach 65°C. As you increase the

sample temperature, the peaks will shift laterally across the screen. This drift in the peak positions will stop when the sample comes to thermal equilibrium at each temperature setting, and this fact can be used as an indication of how long you should wait before taking data at each temperature.

As before, it is useful to make preliminary plots as the data are being obtained; in this case, plot log W versus $1/T$ (K^{-1}). Any data points that deviate seriously from linearity should be repeated if time allows.

CALCULATIONS

For both the isothermal series of runs on samples 1 through 6 and the temperature-dependence runs on sample 1, make a table of your results. For each run, specify the H^+ concentration and/or temperature and list for both methyl band A (pyruvic acid) and band B (dihydroxypropanoic acid) the band position, the FWHM width W (Hz), and the integrated area. If possible, obtain an ASCII file of $I(\nu)$ intensity data, which will allow a least-squares fit to the peaks with a Lorentzian form with baseline corrections; see Exp. 43. This permits a check on the actual line shape and an independent determination of area and width values.

For the constant-temperature data at 25°C, plot πW versus the molar hydrogen-ion concentration. It follows from Eqs. (8) and (18) that

$$\pi W_A = \frac{1}{T_{2A}^*} + k_0^f + k_H^f(H^+) = C_A + k_H^f(H^+) \tag{19a}$$

$$\pi W_B = \frac{1}{T_{2B}^*} + k_0^r + k_H^r(H^+) = C_B + k_H^r(H^+) \tag{19b}$$

where C_A and C_B depend on T but not on (H^+). Thus the slopes of the best linear fits to these plots will yield values for k_H^f and k_H^r and the intercepts $C_{A,B}$ will give estimates of $(1/T_2^*) + k_0$.

Since the integrated area of each methyl band is proportional to the concentration of that solute species, it follows from Eq. (9) that the equilibrium constant $K = (\text{area})_B/(\text{area})_A$. Calculate K values at 25°C from the areas measured on samples 1 through 6. Report a best average value for K at 25°C, weighing the results for various samples differently if that seems appropriate.

Compare the K value obtained above from integrated area data with the value of K calculated from Eq. (10*b*) using your rate constants k_H^f and k_H^r. One can also use Eq. (10*a*) to obtain a rough estimate of the magnitude of the effective T_2 values T_{2A}^* and T_{2B}^* and thus get an idea of the values for k_0^f and k_0^r at 25°C. If one *assumes* $1/T_{2A}^* = 1/T_{2B}^* = C_0$ at 25°C, Eqs. (10*a*), (19*a*), and (19*b*) yield

$$K = \frac{C_A - C_0}{C_B - C_0} \tag{20}$$

Calculate a value for C_0 using the known values of K and C_A, C_B (either the intercepts from your plots or the πW values for sample 1), and then obtain approximate values of k_0^f and k_0^r.

For the high-temperature runs on sample 1, calculate K at each temperature from the integrated area values and plot ln K versus the reciprocal of the absolute temperature. Use Eq. (13) to determine the standard enthalpy change $\Delta\tilde{H}^0$. With the assumption that $\Delta\tilde{H}^0$ is independent of T down to 25°C, calculate an extrapolated value for K(25°C) and compare this to your experimental K value determined at 25°C.

An effort should be made to evaluate the uncatalyzed activation energies E_a^f and E_a^r from the W_A and W_B width data obtained at high temperatures on sample 1. In this case $k_0^f = \pi W_A - 1/T_{2A}^*$ and $k_0^r = \pi W_B - 1/T_{2B}^*$, and your data analysis will depend on what values are assigned to $1/T_{2A}^*$ and $1/T_{2B}^*$. One possibility is to set $1/T_{2A}^*$ and $1/T_{2B}^*$ equal to zero, based on the assumption that their values are negligibly small compared to k_0^f and k_0^r at high temperatures. For this limiting case, make plots of $\ln(\pi W_A)$ and $\ln(\pi W_B)$ versus $1/T$ and use Eq. (12) to determine E_a^f and E_a^r. These values will be lower bounds on the correct activation energies. A second possibility is to assume that $1/T_{2A}^*$ and $1/T_{2B}^* = C_0$ (the value estimated at 25°C). For this case make plots of $\ln(\pi W_A - C_0)$ and $\ln(\pi W_B - C_0)$ versus $1/T$ and determine new values for E_a^f and E_a^r. Compare the difference $(E_a^f - E_a^r)$ obtained both ways with the value of $\Delta\tilde{H}^0$.

DISCUSSION

List the chemical shifts observed in the spectrum of pyruvic acid and comment (qualitatively) on the purity of the acid as inferred from a comparison with literature values.[7] Also note changes in the chemical shifts of the two methyl peaks as a function of H^+ concentration and temperature and suggest a reason for such changes.

Give the standard errors associated with the values of area and width that are determined from the line profile. Is the scatter in the data (K and πW_A, πW_B) as a function of (H^+) or T consistent with those error estimates? Discuss other sources of error beyond line-fit uncertainties. Comment on the agreement between $(\text{area})_B/(\text{area})_A$ and k_H^f/k_H^r as values of K at 25°C. If the temperature dependence of the area ratio had been measured for sample 6 rather than sample 1, would the $\Delta\tilde{H}^0$ value for the acid-catalyzed reaction be the same as $\Delta\tilde{H}^0$ for the uncatalyzed reaction? What difficulty would complicate matters if one tried to determine activation energies from the temperature dependence of the line widths of acid solutions (in addition to the problem of assessing the values of $1/T_{2A}^*$ and $1/T_{2B}^*$)?

On the basis of general concepts from statistical thermodynamics, what would you predict to be the *sign* of ΔS^0 for reaction (1)? Use your data to estimate a value for ΔS^0 at 55°C.

An interesting variation of this experiment involves using the same technique of NMR line-width measurements to study the cis–trans exchange rate in N,N-dimethylacetamide. By determining this rate as a function of temperature over the range 300 to 500 K, one can evaluate the rotational barrier for this cis–trans isomerization.[8]

SAFETY ISSUES

Solution handling should be done wearing gloves, since both pyruvic acid and concentrated HCl can cause skin damage. Use a pipetting bulb; do not pipette by mouth. Dispose of waste chemicals properly.

APPARATUS

NMR spectrometer with peak-integrating and line-width measurement capability; several stoppered bottles for pyruvic acid, HCl, and D_2O; small beaker; six small stoppered tubes or vials for solutions; precision 1-mL graduated pipette; small pipetting bulb; NMR tubes; distillation apparatus for purifying pyruvic acid; refrigerated storage space; pyruvic acid (10 mL); reagent-grade concentrated HCl (3 mL); D_2O (2 mL); fume hood (optional).

REFERENCES

1. R. J. Silbey, R. A. Alberty, and M. G. Bawendi, *Physical Chemistry,* 4th ed., sec. 18.5, Wiley, New York (2005).
2. E. F. H. Brittain, W. O. George, and C. H. J. Wells, *Introduction to Molecular Spectroscopy: Theory and Experiment,* pp. 244–247, 291–293, Academic Press, New York (1970).
3. R. J. Abraham, J. Fisher, and P. Lofthus, *Introduction to NMR Spectroscopy,* Wiley, New York (1992).
4. J. Sandstrom, *Dynamic NMR Spectroscopy,* pp. 6–18, 65–76, Academic Press, New York (1982).
5. P. W. Atkins and J. de Paula, *Physical Chemistry,* 8th ed., p. 538, Freeman, New York (2006).
6. G. Binsch, "Band-Shape Analysis," in L. M. Jackman and F. A. Cotton (eds.), *Dynamic Nuclear Magnetic Resonance Spectroscopy,* Academic Press, New York (1975).
7. C. J. Pouchert and J. R. Campbell, *The Aldrich Library of NMR Spectra,* Vol. II, Aldrich Chemical Co., Milwaukee, WI (1974).
8. F. P. Gasparro and N. H. Kolodny, *J. Chem. Educ.* **54,** 258 (1977).

GENERAL READING

L. M. Jackman and F. A. Cotton (eds.), *Dynamic Nuclear Magnetic Resonance Spectroscopy,* Academic Press, New York (1975).

J. Sandstrom, *Dynamic NMR Spectroscopy,* Academic Press, New York (1982).

EXPERIMENTS IN PHYSICAL CHEMISTRY

EIGHTH EDITION

CARL W. GARLAND
Massachusetts Institute of Technology

JOSEPH W. NIBLER
Oregon State University

DAVID P. SHOEMAKER
(*deceased*)
Oregon State University

McGraw-Hill Higher Education

Boston Burr Ridge, IL Dubuque, IA New York San Francisco St. Louis
Bangkok Bogotá Caracas Kuala Lumpur Lisbon London Madrid Mexico City
Milan Montreal New Delhi Santiago Seoul Singapore Sydney Taipei Toronto

The McGraw-Hill Companies

McGraw-Hill Higher Education

EXPERIMENTS IN PHYSICAL CHEMISTRY, EIGHTH EDITION

Published by McGraw-Hill, a business unit of The McGraw-Hill Companies, Inc., 1221 Avenue of the Americas, New York, NY 10020. Copyright © 2009 by The McGraw-Hill Companies, Inc. All rights reserved. Previous editions © 2003, 1996, 1989, 1981, 1974, 1967, 1962. No part of this publication may be reproduced or distributed in any form or by any means, or stored in a database or retrieval system, without the prior written consent of The McGraw-Hill Companies, Inc., including, but not limited to, in any network or other electronic storage or transmission, or broadcast for distance learning.

Some ancillaries, including electronic and print components, may not be available to customers outside the United States.

This book is printed on recycled, acid-free paper containing 10% postconsumer waste.

1 2 3 4 5 6 7 8 9 0 QPD/QPD 0 9 8

ISBN 978–0–07–282842–9
MHID 0–07–282842–0

Publisher: *Thomas Timp*
Senior Sponsoring Editor: *Tamara L. Hodge*
Director of Development: *Kristine Tibbetts*
Senior Developmental Editor: *Shirley R. Oberbroeckling*
Marketing Manager: *Todd L. Turner*
Senior Project Manager: *Kay J. Brimeyer*
Senior Production Supervisor: *Kara Kudronowicz*
Associate Design Coordinator: *Brenda A. Rolwes*
Cover Designer: *Studio Montage, St. Louis, Missouri*
Compositor: *Laserwords Private Limited*
Typeface: *10/12 Times Roman*
Printer: *Quebecor World Dubuque, IA*

Cover description: The figure depicts the absorption and emission spectra of CdSe nanocrystals, whose color is a sensitive function of size. The figure is based on spectral data provided by NN-Labs. The authors thank both NN-Labs and Evident Technologies for CdSe samples used in the development of the quantum dot experiment.

Library of Congress Cataloging-in-Publication Data

Garland, Carl W.
Experiments in physical chemistry.—8th ed. / Carl W. Garland, Joseph W. Nibler, David P. Shoemaker.
p. cm.
Includes index.
ISBN 978–0–07–282842–9—ISBN 0–07–282842–0 (hard copy : acid-free paper)
1. Chemistry, Physical and theoretical—Laboratory manuals. I. Nibler, Joseph W.
II. Shoemaker, David P. III. Title.
QD457 .S56 2009
541.078—dc22

2007043492

www.mhhe.com